EFFECT OF ANESTHESIA ON CHAOTIC DYNAMICS IN FINGER PLETHYSMOGRAMS

Mayumi Oyama-Higa
Osaka University, Japan

Tiejun Miao
CCI Corporation, Japan

Akira Imanishi
Kwansei Gakuin University, Japan

Junji Kojima
Rakuwakai Otowa Hospital, Japan

Keywords: Chaotech dynamics, Anesthesia, Finger plethysmograms, Non-liner analysis.

Abstract: Chaotic dynamics in finger plethysmogram system was studied in relation to anesthesia processes. The experiments were conducted to observe the changes in finger plethysmogram before, during, and after the anesthesia for a surgery. The largest Lyapunov exponent of the plethysmograms was found to be significant and can be used to correlate the temporal variations of mental/physical status in the processes. There were lower values o f Lyapunov exponents during anesthesia, showing the block effect of anesthesia on central nervous system. There were highly Lyapunov exponents in recovery consciousness from anesthesia. To understand how the chaos arises and to explain the changes in the Lyapunov exponent in finger plethysmograms in experiments, a mathematical model consisting of baroreflex feedback and autonomous interactions was proposed and studied numerically. The decrease of the largest Lyapunov exponent in plethysmograms was explained successfully by the model in relation to the decreased chaoticity, and hence the depressed or blocked central nervous system in higher cerebral region.

1 INTRODUCTION

The chaotic dynamics has been evidenced in experiments in the time series of finger plethysmograms (Sumida et al., 2000). An extensive investigation has focused on applying changes of the deterministic chaos of finger plethysmograms to estimating physiological/physical status (Miao et al., 2003a), diseases diagnosis (Oyama-Higa and Miao, 2005), evaluations of anxiety states (Miao et al., 2003b), and to estimating mental work load by the use of human finger photo-plethysmograms recorded during driving environments. It showed that fluctuation analysis based on chaotic dynamics of the plethysmogram systems could characterize effectively the changes in physical/physiological status in various conditions.

In this study, we designed an experiment to observe the changes in chaos of finger plethysmogram before, during, and after the anesthesia for a surgery. To understand how the chaos changes, a mathematical model was proposed and studied numerically.

2 METHOD OF EXPERIMENTS

The patient participated the experiment was a male aged 71. He was made a deeply anesthesia in order for a surgery of cancer treatment. The surgery taken

Oyama-Higa M., Miao T., Imanishi A. and Kojima J. (2009).
EFFECT OF ANESTHESIA ON CHAOTIC DYNAMICS IN FINGER PLETHYSMOGRAMS.
In *Proceedings of the 4th International Conference on Software and Data Technologies*, pages 400-405
DOI: 10.5220/0002265604000405

place at Rakuwakai Otowa Hospital, Kyoto, December 12, 2008. The participant gave informed consent to all experimental procedures.

The subject slept comfortably in a hospital bed in a relaxed manner. The hand was softly put on the side of his body, held in a relaxed semi-open position, with the palm turned downward. A photoelectric sensor of the plethysmography was placed on the distal phalanx of second finger. Finger plethysmogram was recorded continuously for all processes including before, during and after the surgery, by an instrument (BACS2000; CCI). The signals were digitized with a 200Hz sampling rate with resolution 12 bits, and transferred via an A/D converter to a PC for data processing.

Table 1 shows the steps and processes including before, during and after anesthesia for the surgery.

Table 1: Processes before, during and after the surgery.

9:10	Start	
9:12	Oxygen inhalation	
9:16	Beginning anesthesia	
9:17	Deportation	
9:21	Head Down	
9:22	Inserting Catheter	
9:39	Head Up	t01
9:43	Change O2 to 50%	
		t02
		t03
9:54	Hand move	
10:09	Catecholamine infusion	
10:16	Bbeginning surgery	t04
10:17	Pain stimulation	
		t05
10:23	Pneumoperitoneum	t06
10:30	Arrhythmia	
10:40	Change body position	t07
11:35	Change O2 to 75%	
11:51	Change body position to horizontal	
11:52	Laparotomy	
		t08
12:05	Change O2 to 50%	t09
		t10
		t11
		t12
		t13
		t14
		t15
		t16
		t17
		t18
13:36	Start working closing ventral	t19
13:55	Finished	
13:56	Change O2 to 100%	
14:00	Head Down	
	Bed in horizontal	
14:03	Hand move	t20
	Change O2 to 100%&	
14:11	Atropine sulfate injection	
14:20	Recovery consciousness	t21
14:23	Remove the respirator	
		t22

3 METHOD OF CHAOS ANALYSIS OF TIME SERIES

Given a time series $x()i$, with i=1,..., N, the phase space is reconstructed by using the method of delays. Assuming that we create a d-dimensional phase space using a τ constant delay lag, the vectors in the space are formed by d-tuples from the time series and are given by

$$\boldsymbol{x}(i) = (x(i),..., x(i-(d-1)\tau)) = \{x_k(i)\} \quad (1)$$

where $x_k(i) = x(i-(k-1)\tau)$, with k=1,..., d. In order to correctly reconstruct the phase space, the parameters of delay lag $\boldsymbol{\tau}$ and embedding dimension d should be chosen optimally.

On the reconstructed phase space, one of the important complexity measures is the largest Lyapunov exponent. The Lyapunov exponents characterize how a set of orthonormal, infinite small distances evolve under the dynamics. For a chaotic system, there is at least one positive Lyapunov exponent, let $\lambda_1 > 0$ be the largest exponent. The defining property of chaos is sensitive dependence on initial conditions, in the following sense. Given an initial infinite small distance

$\Delta x(0)$, its evolution obeys

$$\Delta x(t) = \Delta x(0) e^{\lambda_1 t} \quad (2)$$

For an M-dimensional dynamical system, there are M Lyapunov exponents. We estimated only λ_1 using algorithm of Sano and Sawada (Sano and Sawada, 1985).

We used chaos analysis to finger plethysmograms and estimate the largest Lyapunov exponent λ_1.

4 EXPERIMENT RESULTS

Since the chaoticity of the plethysmogram can give important information about human temporal processing, we used chaos analysis to the plethysmograms and estimate the largest Lyapunov exponent. Parameters used are embedding dimension d=4, time delay lag is taken as 50ms. Fig.1 illustrates changes of the largest Lyapunov exponent for all processes on the Table I, where times indicated ranged from t1-t22.

There are changes of chaotic dynamics indicated by Lyapunov exponent during all experiment processes. We found there smaller values estimated

during t11 to t19, showing the effect of laparotomy and change O2 to 50% on cam down the mental/physical status. Whereas there were largely arising Lyapunov exponents in recovery consciousness from anesthesia, even higher than the ones in initial stage before the surgery. There were overall lower values o f Lyapunov exponents than the average one for healthy subject that had averaged values ranged 3-5, showing the block effect of anesthesia on central nervous system.

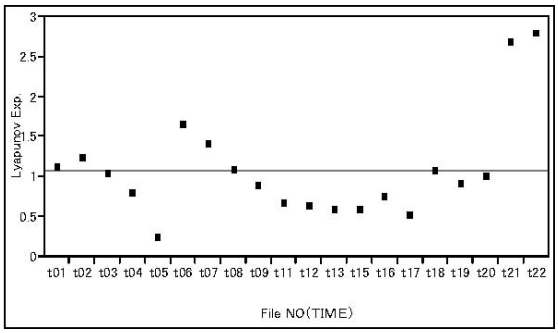

Figure 1: Lyapunov exponents for experimental processes.

5 MATHEMATICAL MODEL AND SIMULATIONS

To understand emergence of changes of chaos in the finger plethysmograms in the experiments, a mathematical model is proposed. Fig. 2 shows a schematic description of the model used in this paper. The model consists of a feedback loop and physiological factors (Miao et al., 2006). The pressure receptors are the sensors of the system, which senses and transmits neural afferents from pressure to cardio-vascular centre. Neural efferents are created and then sent to effectors. There are influences both from respiratory centers and from higher cerebral region.

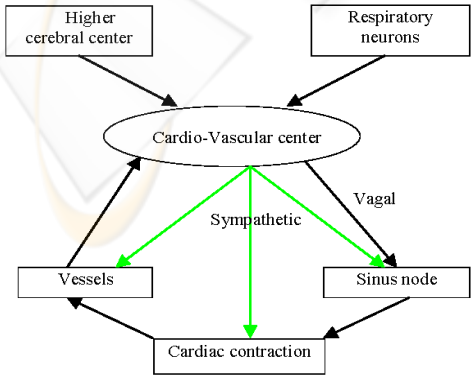

Figure 2: Schematic representation of the model.

It notes that pulsations in blood volume of ear were able to be represented as a response function to pulsations in radial artery (Liu, 2003), and whence a proportional relation between the finger plethysmogram and artery blood pressure can be approximately assumed. Thus, for sake of simplifying unimportant details, our model concentrated on dynamics of blood pressure in a well approximation to approaching finger plethysmograms without loss of generality.

In the model, baroreceptor activity is determined by pressure p and its derivative, with constants k_1=0.02 mm/Hg, k_2=0.00125 smm/Hg, and p_0=50mmHg, as

$$V_b = k_1(p - p^{(0)}) + k_2 \frac{dp}{dt} \quad (3)$$

The neural efferent of sympathetic activity is determined by (3) as

$$V_S = \max(0, v_S^{(0)} - k_S^b v_b + k^r(1 - \cos(2\pi r)) + \gamma Y) \quad (4)$$

where constants v =0.8, k_s =0.7 , k^r =0.035; Y is the impulse input from higher cerebral center and is assumed to only affect sympathetic neural efferents through a coupling coefficient γ. r is an instance phase of respiration describing effects of respiration modulations. Likewise, efferent parasympathetic activity is determined by (3) as

$$v_p = \max(0, v_p^{(0)} + k_p^b v_b + k^r(1 - \cos(2\pi r))) \quad (5)$$

where constants $v^{(0)}$=0.0, k^b =0.3 .

As suggested in Kotani (Kotani et al., 2005), the instance respiration phase r has a constant phase velocity during inspiration with period T_{resp}=4.5s, as

$$\frac{dr}{dt} = \frac{1}{T_{resp}} \quad (6)$$

Whereas during expiration (sin(2 πr) >0) and if v >v, r is modulated by baroreceptor afferents as

$$\frac{dr}{dt} = \frac{1}{T_{resp}} - G(v_b - v_{trig}) \quad (7)$$

where G=0.2, v_{trig} =1.3 .

The pulsating heartbeat is generated by an integrate-and-firing model. A pacemaker phase of sinus node was introduced. A new heartbeat is generated when the phase reaches a threshold of 1.0. At this point the phase is then reset to zero. The phase velocity is determined by sympathetic and parasympathetic influences on sinus node by the relation

$$\frac{d\phi}{dt} = \frac{1}{T^{(0)}} f_S f_P \quad (8)$$

Where $T^{(0)}$=1.1s, and

$$f_s = 1 + k_\phi^{cNe}\left(c_{cNe} + (\hat{c}_{cNe} - c_{cNe})\frac{c_{cNe}^{n_{cNe}}}{\hat{c}_{cNe}^{n_{cNe}} + c_{cNe}^{n_{cNe}}} \right) \quad (9)$$

$$f_p = 1 - k_\phi^p\left(v_p(t-\theta_p) + (\hat{v}_p - v_p(t-\theta_p))\frac{v_p^{n_p}(t-\theta_p)}{\hat{v}_p^{n_p} + v_p^{n_p}(t-\theta_p)} \right) F(\phi) \quad (10)$$

where sympathetic influence *f*s is determined by constants of $k_\phi^{cNe} = 1.6$, $\hat{c}_{cNe} = 2.0$, n_{cNe}=2., and cardiac concentration (*ccNE*) of neurotransmitter "norepinephrine" (*Ne*). The cardiac concentration (*ccNe*) follows kinetics equation:

$$\frac{dc_{cNe}}{dt} = -\frac{c_{cNe}}{\tau_{cNe}} + k_{c_{cNe}}^s v_s(t - \theta_{cNe}) \quad (11)$$

Where t_{cNe}=2.0, $K_{c_{cNe}}^S$ =1.2, and time delay θ_{cNe}=1.65s (default) due to the neural conduction. The parasympathetic influence *f*p is determined by constants k_φ^p = 5.8, $\hat{v}_p$= 2.5, *np*=2.0, and time delay θ_p =0.5s (default=. The influence of *f*p is fast and therefore does not need transmitter kinetics. Whereas phase effective cure $F(\phi)$ is added in (10) by

$$F(\phi) = \phi^{1.3}(\phi - 0.45)\frac{(1-\phi^3)}{(1-0.8)^3 + (1-\phi)^3} \quad (12)$$

Blood pressure during the systolic part of the heart cycle is determined by diastolic pressure of the previous beat d_{i-1} and cardiac contractility S_i of the current beat:

$$p = d_{i-1} + S_i \frac{t - t_i}{t_{sys}} \exp\left\{ 1 - \frac{t - t_i}{t_{sys}} \right\} \quad (13)$$

where t_i is the time of last contraction onset, t_{sys} = 0.125s , and cardiac contractility, according to Frank-Starling law, is

$$S'_i = S^{(0)} + k_s^c C_{cNe} + k_s^t T_{i-1} \quad (14)$$

Cardiac contractility with saturation becomes

$$S_i = S'_i + (\hat{S} + S'_i) + \frac{S'^{ns}_i}{S'^{ns}_i + \hat{S}^{ns}} \quad (15)$$

Where $S^{(0)}$=25mmHg, k_s^c =40mm/Hg, k_s^t =10mm/Hg, $\hat{S}$ =70mmHg, *ns*=2.5. Blood pressure during diastolic part of hear cycle, according to relaxation of Windless arteries, is

$$\frac{dp}{dt} = -\frac{p}{t_v(t)} \quad (16)$$

Where relaxation constant t_v is determined by vascular concentration of C_{vNe}:

$$\tau_v = \tau_v^{(0)} - \tilde{\tau}_v\left(c_{vNe} + (\hat{c}_{vNe} - c_{vNe})\frac{c_{vNe}^{n_{vNe}}}{\hat{c}_{vNe}^{n_{vNe}} + c_{vNe}^{n_{vNe}}} \right) \quad (17)$$

where $t_v^{(0)}$ τ= 2.2s, $\hat{t}_v$ = 1.2*s* , c_{vNe}= 10.0, n_{vNe}= 1.5 , and vascular concentration follows equation of

$$\frac{dc_{vNe}}{dt} = -\frac{c_{vNe}}{t_{vNe}} + k_{c_{vNe}}^s v_s(t - \theta_{vNe}) \quad (18)$$

Where time delay θ_{vNe} =1.65s (default) is due to neural conduction t_{vNe} =2.0, and $k_{c_{vNe}}^s$ =1.2.

Because the higher cerebral activity played important in modulation central nervous system and autonomic system, our model added the influences to sympathetic neural efferent activity through a coupling coefficient γ as shown in (4). Dynamics of the cerebral activity was assumed to be described by Duffing equation that was able to generate both limit cycle and chaotic behavior (Bergey and Franaszczuk, 2001), as evidenced experimentally by measurements of electroencephalography (EEG). Thus, we chose Duffing equation to describe cerebral impulse activities Y as:

$$\frac{d^2Y}{dt^2} + \varepsilon\frac{dY}{dt} + aY + bY^3 = B\cos\omega t \quad (19)$$

Where ε =0.05, a=0, b=1.0, ω=1.0, B=7,5. This setting of parameters gives arise of chaotic dynamics in agreement with studies on human brain (Korn and Faure, 2003).

In simulation studies, we used a Runge-Kutta method to make numerical simulations of the delay-differential equations. Ring buffers were used to handle time delays in equations. We used the initial values of *p*=110 mmHg, $c_{cNe} = c_{vNe}$ =0.15, d_0=90 mmHg, S_0=40 mmHg, and T_0=1.1s. Simulations were performed to skip first 200s transients and recorded the following data.

For parameters γ =0.1, θ_{cNe} =2.5s, in Fig. 3 we calculated and depicted temporal variations of blood pressure *p*, concentrations c_{cNe}, higher cerebral activity *Y*, baroreceptor activity v_b, delayed sympathetic activity v_s (t- θ_{cNe}), delayed vagal activity $v_p(t-\theta_p)$, and phase of cardiac pacemaker φ. There appeared a complex dynamics in blood pressure *p*. Indeed, as shown in Fig. 4, return maps for peak value of blood pressure P_i showed

complexity and random-like patterns, characterizing a chaotic behavior.

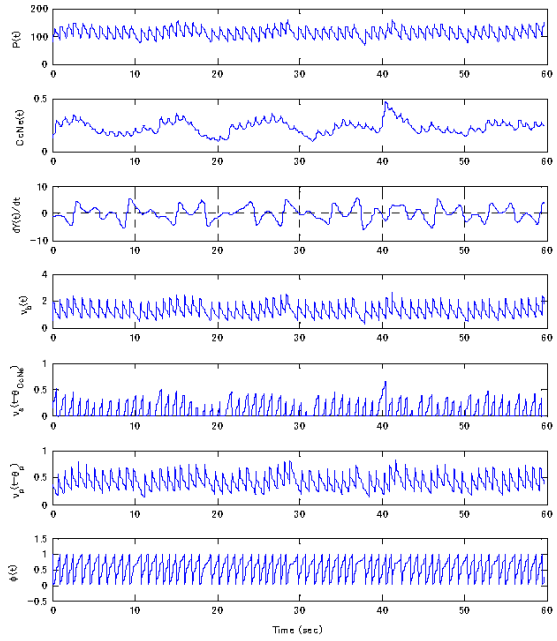

Figure 3: Output with influence of higher cerebral center.

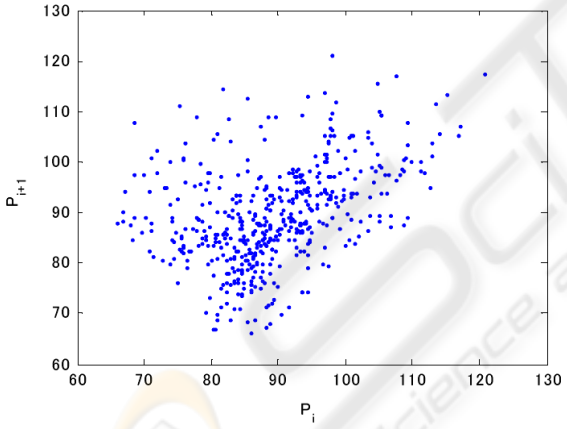

Figure 4: Return maps for peak value of pressure P_i.

Additionally the reconstructed orbits (called attractor) exhibited complex, non-periodic, diverse orbiting patterns, strongly suggesting deterministic chaotic behaviors. Lyapunov exponents of the chaotic attractors were also calculated, as described in next section, and showed positive values, again being consistent with chaotic behaviors.

Higher cerebral center influence, therefore, was found to play an important role and largely responsible for emergence of chaos in finger plethysmograms.

Furthermore, effects of chaoticity in higher cerebral center were studied by simulation to understanding how it affects the baroreflex controlled cardiovascular system. Keeping coupling coefficient γ =0.1 in constant, while changing parameter *B* to 6.6, 7.0, and 7.5, we obtained a changing chaoticity of higher center activity described by Duffing equation (19), which was characterized by changing Lyapunov exponents. The largest Lyapunov exponents of (19) were λ_1=0.066, 0.105, 0.078, corresponding to three parameters of *B*. Putting these parameters into the model, we obtained time series of blood pressure *p*. The largest Lyapunov exponent was then computed using Sano and Sawada algorithm (Sano and Sawada, 1985). Fig. 5 plotted these results, showing a well linear relationship between the largest Lyapunov exponents of higher cerebral center and ones of blood pressure *p*.

This relation shown in Fig.5 explains theoretically the causes for an increase in chaos of finger plethysmogram come from higher Lyapunov exponent in higher cerebral center. In other words, there is higher information processing in central nervous system, leading to increasing complexity of finger plethysmograms.

6 CONCLUSIONS

Chaotic dynamics in finger plethysmogram system was studied in relation to anesthesia processes. The largest Lyapunov exponent of the plethysmograms was found to be significant and can be used to characterize the changed in mental/physical status for the experimental processes. There were lower values o f Lyapunov exponents, indicating a blocked or depressed effect of anesthesia on central neural system. We found there a further smaller values estimated during the laparotomy and change O2 to 50%, showing the effect of cam down on mental status. Whereas there was a highly Lyapunov exponent in recovery consciousness from anesthesia, even higher than the period of time before preparation of the surgery.

To understand how the chaos arises and to explain the changes in the Lyapunov exponent in finger plethysmograms in experiments, a mathematical model consisting of baroreflex feedback and autonomous interactions was proposed and studied numerically. By using of the model, the decrease of the largest Lyapunov exponent in plethysmograms was explained in relation to the decreased chaoticity, and hence the depressed or blocked central nervous

system in higher cerebral region. Highly arising values of Lyapunov exponent was theoretically explained as caused from excitations in activities underlying central nervous system.

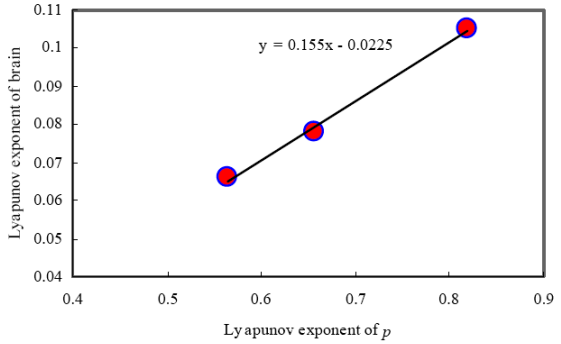

Figure 5: A plot of the largest Lyapunov exponent of blood pressure with respect to one of higher cerebral center.

ACKNOWLEDGEMENTS

We would like to deeply thank Dr. Maho Imoto, Rakuwakai Otowa Hospital, who provided with useful and helpful assistance during the experiments.

REFERENCES

Sumida, T., Y. Arimitu, T. Tahara, and H. Iwanaga, "Mental conditions reflected by the chaos of pulsation in capillary vessels", Int J Bifurcation and Chaos, Vol.10, 2245-2255, 2000.

Miao, T., T. Shimizu, and O. Shimoyama, "The use of chaotic dynamics in finger photoplethysmography to monitoring driver mental workload", JSAE Annual Congress, Japan, No.18-03, 2003a.

Oyama-Higa, O. and T. Miao, "Representation of a physiopsychological index through constellation graphs", Lecture Notes in Computer Science, Springer-Verlag GmbH. Vol.3610, 811, 2005.

Miao, T., G. Higashida, W. Miyazaki, H. Asaoka, "Prognosis for drug treatment based on chaotic dynamics of human finger photoplethysmograms", Jpn J Appl Physiol, Vol.33, 183-189, 2003b.

Sano, M. and Y. Sawada (1985). Measurement of the Lyapunov spectrum from a chaotic time series, Phys Rev Lett, Vol.55, p1082

Miao, T., O. Shimoyama, and M. Oyama-Higa (2006). Modelling plethysmogram dynamics based on baroreflex under higher cerebral influences, IEEE International Conference on Systems, Man, and Cybernetics, Oct.8-11, 2006 Taiwan, p.2885-2890.

Liu, J. (2003). Establishment of finger microcirculation volume blood flow model and estimation of model parameters, J Beijing Institute Civil Eng. and Architecture, Vol.20, p45-51

Bergey, G. K and P. J. Franaszczuk (2001). Epileptic seizures are characterized by changing signal complexity, Clinical Neurophysiology, Vol.112, p241-249.

Korn, H. and P. Faure (2003). Is there chaos in the brain? II. Experimental evidence and related models, C R Biologies, Vol.326, 787-840.

Kotani, K., Z. R. Struzik, K. Takamasu, H. E. Stanley, and Y. Yamamoto (2005). Model for complex heart rate dynamics in health and diseases, Phys Rev E, Vol.72, p041904